

High- performance MALDI-TOF Imaging Mass Spectrometry of proteins for detection and identification of single cells

Marvin Vestal and Kevin Hayden

SimulTOF Systems

Abstract

A new high performance linear MALDI-TOF mass spectrometer is applied to imaging both proteins and lipids in porcine pancreatic tissue. This work employs, a 10 μ m diameter laser beam operated at rates up to 5 kHz. The protein spectra were acquired by rastering the 10 μ m laser at 2 mm/s at intervals of 10 μ m, and the laser was operated at 200 Hz giving 1 laser shot per 10 μ m pixel. The lipid spectra were acquired using the same rastering parameters, but the laser was operated at 2 kHz giving 10 shots per 10 μ m pixel. In both cases intense spectra were observed corresponding to the Isles of Langerhans.¹ Some pixels demonstrate detection of single alpha and beta cells that produce glucagon and insulin, some that appear to correspond to a fourth type of islet cell, the F (or PP) cell located at the periphery of the islets and secretes pancreatic polypeptide (although the mass of the polypeptide detected, 4395 Da, is higher than literature value for other organisms). Spectra were acquired at a rate of 200 pixels/s and the total area of the pancreas section was about 22 mm² producing a total of 220,000 spectra. This is not the first example of MALDI-TOF imaging of proteins at 10 μ m spatial resolution over a full tissue section, but it is far faster than earlier results. One of the predicted C-peptides, MW 2900, was detected in the beta cells, but the intensity relative to insulin was variable. The islets of Langerhans also include delta cells that produce somastatin; these were not detected.

Introduction

Laser-based desorption ionization techniques have been developed for Imaging Mass Spectrometry (IMS) to provide spatial localization and relative abundance of multiple biomolecules directly from tissue sections². For MALDI, several thousand mass spectra may be acquired directly from a tissue sample and the spatial distribution of each signal can be plotted to produce hundreds of ion images in a single experiment. This type of specific molecular imaging does not require antibodies or other target specific reagents. Although MALDI IMS has proved to be a very powerful technology, previous work has required very long acquisition times to provide high spatial resolution imaging of whole tissue sections. In one recent example of imaging a complete tissue section at 10 μ m spatial resolution the laser was operated at 500 Hz and 80 shots were acquired for each pixel.³ This corresponds to 6.25 pixels/s for a total of 44.44 hours/cm² for each image.

In earlier work⁴ specific primary antibodies were conjugated to small reporter mass tags (\sim m/z 500) that were used to localize neuroendocrine markers in human pancreatic islet. However, the intracellular expression of these markers could not be achieved⁵. The typical size of human pancreatic islets ranges from 25 μ m to 400 μ m and the diameter of a single endocrine cell is approximately 10 μ m. MALDI Imaging Mass Spectrometry has been used for in situ proteomic analysis of preneoplastic lesions in pancreatic cancer.⁶ In this work MALDI mass spectra were measured with a spatial resolution of 70 μ m

in linear mode. Ions were detected in a mass range of m/z 2500 to 25000. Targeted multiplex Imaging Mass Spectrometry employs photocleavable mass tag bound to an antibody wherein the low molecular weight mass tag can be readily ionized by laser desorption ionization mass spectrometry. This technique has targeted single cells within tissue using transmission geometry laser desorption ionization mass spectrometry with a 2 μm diameter laser spot irradiating the biological specimen.⁷ This work demonstrated detection of single beta cells, but the total area imaged was 100x100 μm corresponding to the area of a relative small Islet of Langerhans.

Description of instrument

This work employed a new SimulTOF TWO linear MALDI-TOF with 1400 mm flight path and programmable voltages that provides isotopic resolution for peptides and metabolites below 4 kDa, and isotopic envelope resolution for high masses. This instrument employs a new ion optics system with grounded ion source and efficient transfer and detection of ions over a broad mass range that provides very high sensitivity, precision, and dynamic range for both positive and negative ions. The instrument employs a solid-state Nd:YLF laser that provides 349 nm photons with fluence up to 30 μJ at 5kHz. The laser spot size is manually adjustable from 10 to 50 μm , and was set at 10 μm for this work. The fluence delivered to the sample was approximately 3 μJ with the sinapinic acid matrix used for protein imaging. A new 8 Bit High Speed Digitizer with an ADC sampling rate up to 2.5 GS/s on a single channel is employed.⁸ This digitizer features a PCI Express interface and optimized drivers that enable data transfer rates in excess 3.4GB/s. Software has been developed and validated so that complete spectra can be acquired, stored and analyzed at rates greater than 300 spectra/s.

The present work represents one of the first tests of this system. Protein spectra were acquired over the mass range 500-30,000 Da at an acquisition rate of 200/s. Typewriter mode was used wherein spectra were only saved when scanning from left to right. This reduced the effective speed to 130 spectra/s.

Materials and Methods for Sample Preparation and Matrix deposition

Chloroform, ethanol, Sinapinic acid and tert-butanol were purchased from Sigma-Aldrich (Milwaukee, WI); acetic acid was purchased from VWR scientific (Philadelphia, PA) and stainless steel sample holder from SimulTof systems (Marlborough, Ma).

Carnoy's solution was prepared from 27 mL of ethanol, 13.5 mL of chloroform and 4 mL of acetic acid. Fresh Frozen Porcine pancreas 12 μm tissues sections were supplied pre- mounted onto ITO coated microscope slides by Prof Ron Heeren European institute for molecular imaging, (M4I) at Maastricht University Netherlands stored in a -20°C freezer.

Rinsing procedure

Removal of lipids by mean of rinsing the tissue sections on the slide is essential to obtain optimal sensitivity and high quality protein ion images. This is achieved using the following 6 step rinse protocol⁹

- Rinse slide in 70% ethanol for 30 seconds
- Rinse slide in 100% ethanol for 30 seconds
- Rinse slide in Carnoy's fluid for 2 minutes
- Rinse slide in 100% ethanol for 30 seconds
- Rinse slide in 40% ethanol for 30 seconds
- Rinse slide in 100% ethanol for 30 seconds

Tissue sample were transferred to a vacuum oven (VWR model 1400e) to dry at < -30 in/hg for 20 minutes.

Matrix sublimation procedure

150 mg of Sinapinic acid was uniformly distributed in a 1.5 cm X 4 cm array at the bottom of the sublimation chamber (Ace Glass Incorporated, model 8023-55) outer body section. The ITO slide with tissue section was tapped to the underside of the upper body of the sublimation chamber top using ¼ inch strips of copper tape. Next the upper body outer reservoir of the sublimation chamber was filled with 400 mL of water and ice. Finally the chamber was sealed and pump down to < -30 in/hg of vacuum, using a hot plate (Waage Electric Stove, model D6A-12-1) the sublimation chamber was heated in the following sequence; 125°C for 3-1/2 minutes, 150°C for 7 minutes, 175°C for 4 minutes and 185°C for 15 minutes. After the final 15 minute duration the ITO slide with tissue section was removed from the sublimation chamber in preparation for the recrystallization step.

Matrix recrystallization conditions

A recrystallization chamber was configured using 2 top covers from 100mm petri dishes. The sublimated ITO slide with tissue section was mounted onto a SimuTof sample plate holder. The sample plate holder was then placed onto the underside of one of the petri dish top covers with tissue section facing down, 6 neodymium-iron-boron rare-earth magnets (Magcraft, model nsn0579) positioned on the outside of the top cover were used to hold the sample plate holder into position. Chromatography paper (Whatman, Cat No: 3030-6185) what cut to a 30mm X 75mm section and placed in the bottom of the second petri dish top cover. 1mL mixture consisting of 880uL tert-butanol and 120uL of milli Q water was uniformly deposited on to the chromatography paper. The 2 petri dish top covers were joined together and sealed using common laboratory tape. Next the apparatus was then placed in to a lab oven (VWR, model 1350 gm) preheated to 79°C for 2 minutes. The sample plate holder was removed from the apparatus allowed to dry for 5 minutes. Finally the sample plate holder with tissue section was loaded into the mass spectrometer for analysis.

Results

This project was initiated to evaluate the speed and performance of the new MALDI-TOF imaging technology described above. The results presented here comprise a progress report, but do not represent the ultimate speed that can be achieved. The protein spectra were acquired by rastering the 10 µm laser at 2 mm/s at intervals of 10 µm, and the laser was operated at 200 Hz giving 1 laser shot per 10 µm pixel. The lipid spectra were acquired using the same rastering parameters, but the laser was

operated at 2 kHz giving 10 shots per 10 μm pixel. In both cases intense spectra were observed corresponding to the Isles of Langerhans.

MALDI Images of proteins in porcine pancreas are shown in Figure 1. The area imaged was a rectangle approximately 7 mm wide by 6 mm high that was substantially larger than the tissue section. An image generated from total ion current (TIC) for mass range 2-20 kDa with zero threshold is shown in Figure 1A for a total of 415,565 spectra acquired in 54 minutes. Area imaged is 41.5565 mm^2 but the total area of the tissue section is approximately 22 mm^2 as shown by the camera image in **B** and **C**; thus if we had scanned only over the tissue section, the image could have been generated in less than 30 minutes.

Figure 1A and 1B are presented in heat-map mode where red indicates high intensity and blue low intensity, and Figure 1C shows the images superimposed of masses 5778 and 3484 corresponding to porcine insulin and glucagon, respectively, corresponding to the beta and alpha cells of the Islets of Langerhans that produce insulin and glucagon. An expanded image of largest Islet detected (Islet 3 at upper left in the overall image) is shown in Figure 1D. The nine largest Islets of Langerhans are labeled in Figure 1C with the number indicating the order in the vertical direction.

An alternative display of the image data is presented in Figure 2 where the intensities of m/z 5788 (green) and 3484 (red) are plotted in order of acquisition. Each scan in the horizontal direction generates 700 spectra; thus Acquisition # divided by 700 corresponds to vertical distance from the top measured in 10 μm pixels. The Islet numbering is shown in Figure 1C, and the expansion in the upper panel corresponds to the same data for Islet 3 as shown as the expanded image in Figure 1D. The advantage of this display is that the intensity of the ions detected in each pixel is more accurately shown than is possible with the two-dimensional map. Expanded views of three consecutive passes across pixel 3 are shown in Figure 3. The upper panel shows the intensities detected in individual pixels and some appear to correspond to individual beta cells.

The upper panel in Figure 4 shows the portion of the full image that includes Islet 1, and the lower panel shows intensities of all of the spectra from Islet 1, and a portion of the spectra from Islet 2 that are scanned within the vertical distance indicated by the red lines in the upper panel. Figure 5 shows an expanded view of 6 passes across Islet 1 from near top (upper left) to near bottom(lower right).

The arrow in Figure 2 indicates what appears to be a single isolated beta cell. An expanded view of that portion of the 1-dimensional image is shown in Figure 6 along with spectra of 3 consecutive pixels. This appears to represent a single beta cell that located at the boundary between the 2 pixels.

A fourth type of islet cell, the F (or PP) cell, is located at the periphery of the islets and secretes pancreatic polypeptide. We detect a polypeptide at m/z 4396 that is present primarily in the islet periphery, but the mass is about 200 Da higher than indicated in the literature. Two dimensional images for this ion (blue), insulin (green) and glucagon (red) are shown for several of the Islets in Figure 7, and 4396 is clearly present except in some very small clusters that appear to be almost exclusively beta cells.

A C-peptide at m/z 2901 is also detected in the Islets. The map of this peptide is similar to that for insulin, but the ratio is variable. Heat maps for each of the 4 major masses detected in the Islets are

shown for Islet 3 in Figure 8, and single shot mass spectra for selected single pixels are shown in Figure 9. These 4 major ions are almost exclusively detected in the islets; some examples of protein mass spectra from other portions of the pancreas are shown in Figure 10. The islets of Langerhans also include delta cells that produce somastatin; these were not detected.

A lipid image from a different porcine pancreatic tissue section is shown in Figure 11. The Isles of Langerhans are readily distinguished in this image, but these data do not appear to be specific to individual cells. Lipid image and spectrum from an Islet of Langerhans (left) and another portion of the pancreas (right) are shown in Figure 12. We asked Professor Robert Murphy, a recognized authority on molecular imaging of lipids, for his views on the value of this work and he responded as follows:

“I may enthusiastically speak of the cellular resolution you have been able to demonstrate with the imaging of the islet in terms of the specific phospholipids that are present in the islet cell. After a lot of micro-dissection effort there has been evidence accumulating that rather specific phospholipid molecular species of polyunsaturated fatty acids are associated with the islets. What you now show is that PC(36:5) and PC (38:5) are present in islet membranes at remarkable concentrations, at m/z 780.6 and 808.6 respectively. Analysis by negative tandem mass spectrometry will reveal exactly the molecular species present. This opens the way for new hypotheses and directions of research. I for one would love to see pancreas imaged by your new instrument from animals that have been made diabetic and insulin dependent. I think the phospholipid content will be quite interesting and different.”

Conclusion and future work

We have showed the ability to detect and characterize single cells, and small clusters of cells by rapidly imaging whole tissue sections where the location of these cells of interest may not be detected by classical staining and imaging. The Isles of Langerhans provide an excellent example, and we are interested in collaborating on additional work involving pancreas of other species, as well as other organs. Perhaps more importantly we would like to explore detecting and characterizing cancer cells that may show a different molecular signature than the surrounding tissue. Some organs with larger tissue sections, for example porcine liver, with total area of 1.6 cm^2 have been imaged producing 1.6 million pixels; the resulting data files are very large and software improvements are currently being tested to manage these huge files. Software has been developed and validated so that complete spectra can be acquired, stored and analyzed at rates greater than 300 spectra/s. This new software makes it possible to process the raw spectral data “on the fly” to carry out processes including smoothing, baseline correction, peak detection, and recalibration without sacrificing speed making it practical to save peaks and discard the raw data. As a result the files are reduced in size by about an order of magnitude, and time required for producing images is also greatly reduced.

The protein image was obtained using a single $10 \mu\text{m}$ dia laser shot for each $10 \mu\text{m}$ pixel. This measurement was repeated over the same sample using precisely the same acquisition parameters as the first acquisition, and the two images are virtually identical indicating that there is no detectable

depletion of the sample from a single shot with the laser fluence used for these measurements. The small differences that can be observed appear to be mainly statistical as expected for single shot spectra and indicate that precision of both intensity and mass can be improved by averaging more laser shots. Scanning the sample at 3 mm/s with a laser rate of 4.8 kHz provides 16 shots/pixel for 10 μm pixels at 300 pixels/s. More laser shots per pixel requires reducing the scan rate, and the optimum laser fluence and laser shots/pixel will be explored for trade-offs between speed and precision. When more than one laser shot per pixel is employed, $\frac{3}{4}$ of the ions detected are from material in the particular pixel and $\frac{1}{8}$ from the adjacent pixels. This corresponds to a small smoothing of the image along the rastered coordinate, but does not significantly affect the ability to detect single cells with dimensions similar to the pixel size. We have recently modified the laser focusing optics to produce a laser beam 5 μm in diameter, and we plan to repeat these measurements with higher spatial resolution.

References

1. Jaitley S and Saraswathi TR, Pathophysiology of Langerhans cells; J Oral Maxillofac Pathol. 2012 May-Aug; 16(2): 239–244.doi: [10.4103/0973-029X.99077](https://doi.org/10.4103/0973-029X.99077)
2. Caprioli RM, Farmer TB, Gile J. Molecular imaging of biological samples: localization of peptides and proteins using MALDI-TOF MS. *Anal Chem*. 1997; 69(23):4751–60. [PubMed: 9406525]
3. Anderson DMG, Spraggins JM, Rose KL, Schey KKL; High Spatial Resolution Imaging Mass Spectrometry of Human Optic Nerve Lipids and Proteins; *J. Am. Soc. Mass Spectrom*. (2015) DOI: 10.1007/s13361-015-1143-9
4. Thierry G, Shchepinov MS, Southern EM, Audebourg A, Audard V, Terris B, Gut IG. Multiplex target protein imaging in tissue sections by mass spectrometry - TAMSIM. *Rapid Commun Mass Spectrom*. 2007; 21(6):823–9. [PubMed: 17294518]
5. Thierry G, Anselmi E, Audebourg A, Darii E, Abarbri M, Terris B, Tabet JC, Gut IG. Improvements of Targeted multiplex mass spectrometry IMAGING. *Proteomics*. 2008; 8(18):3725–34. [PubMed: 18780398]
6. Gruner BM, Hahne H, Mazur PK, Trajkovic-Arsic M, Maier S, Esposito SI, Kalideris E, Michalski CW, Kleeff J, Rauser S, Schmi RM, Bernhard K, Walch A, Siveke JT; MALDI Imaging Mass Spectrometry for In Situ Proteomic Analysis of Preneoplastic Lesions in Pancreatic Cancer; *PLoS ONE* www.plosone.org 1 June 2012 | Volume 7 | Issue 6 | e39424.
7. Lavenant G, Zavalin A, and Caprioli R M; Targeted Multiplex Imaging Mass Spectrometry in Transmission Geometry for Subcellular Spatial Resolution; *J Am Soc Mass Spectrom*. 2013 April ; 24(4): 609–614. doi:10.1007/s13361-012-0563-z.
8. New Spectrum Instruments M4i Series.
9. Junhai Yang and Richard M. Caprioli. *Anal Chem*. 2011 July; 83(14):5728-5734
10. Robert C. Murphy, Ph.D., University Distinguished Emeritus Professor, Department of Pharmacology, University of Colorado Denver; private communication

Figures

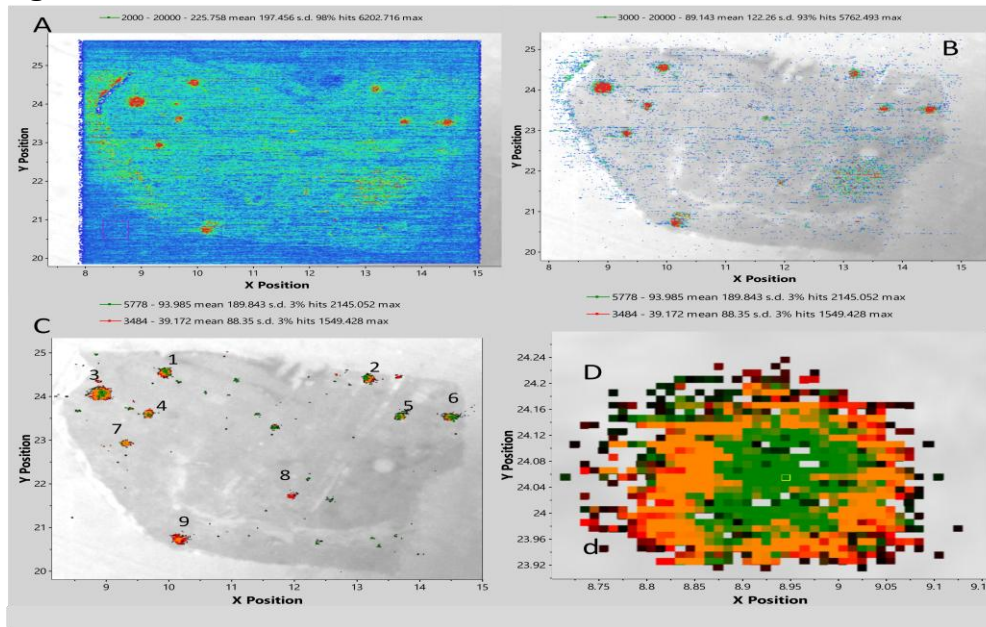


Figure 1. MALDI Images of porcine pancreas. **A** total ion current (TIC) for mass range 2-20 kDa with zero threshold with all 415,565 spectra displayed. Area imaged is 41.5565 mm² but the total area of the tissue section is approximately 22 mm² as shown by the camera image in **B** and **C**. Expanded image **D** of largest Isle at upper left in the overall image. The nine largest Islets of Langerhans are labeled in **C**.

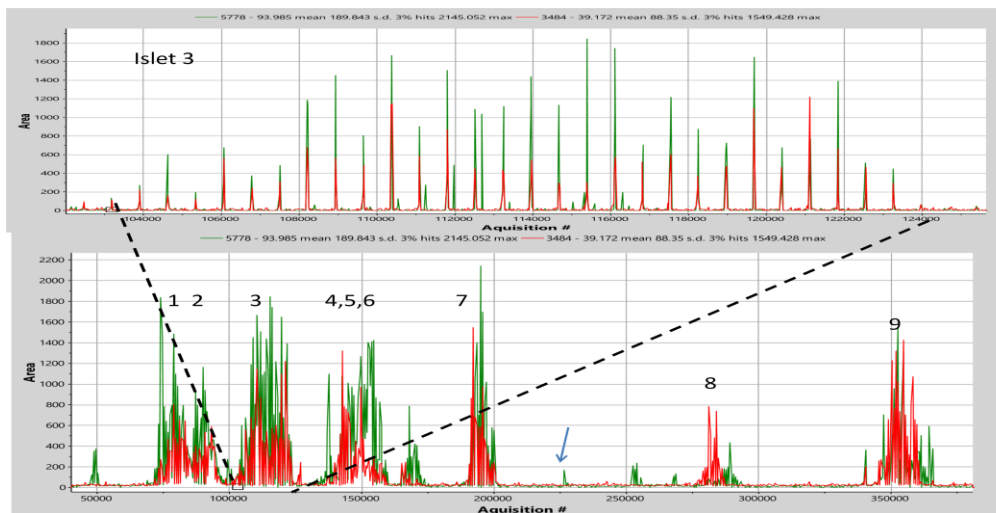


Figure 2. One dimensional display of the intensities of MH⁺ 5778 (green) and 3484 (red) corresponds to molecular ions for insulin and glucagon. Each scan in the horizontal direction generates 700 spectra; thus Acquisition # divided by 700 corresponds to vertical distance from the top measured in 10 μ m pixels. The Islet numbering is shown in Figure 1C and the expansion corresponds to Islet 3 shown as the expanded image in Figure 1D. Arrow indicates what appears to be a single isolated beta cell.

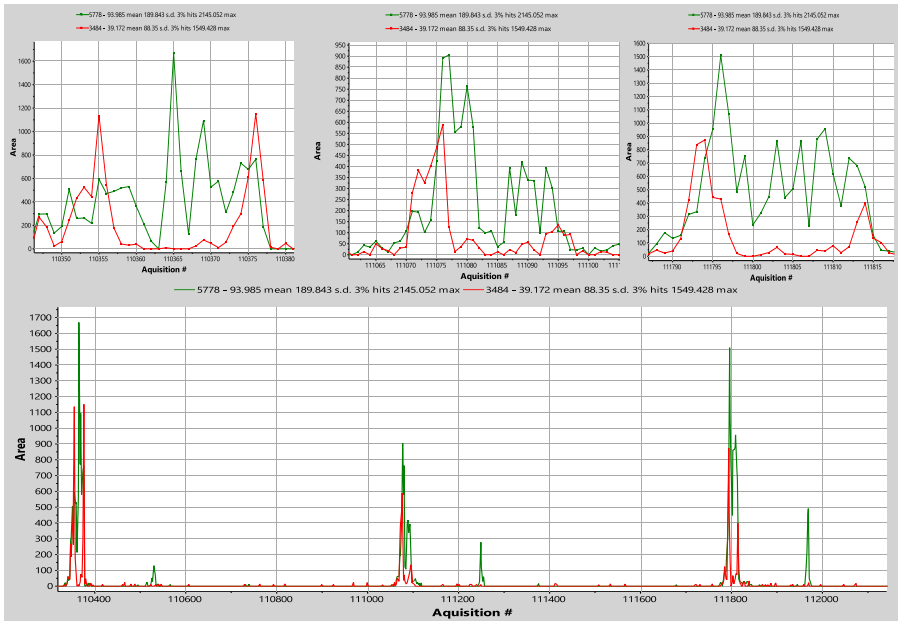


Figure 3. Expanded views of 3 consecutive passes across Islet 3.

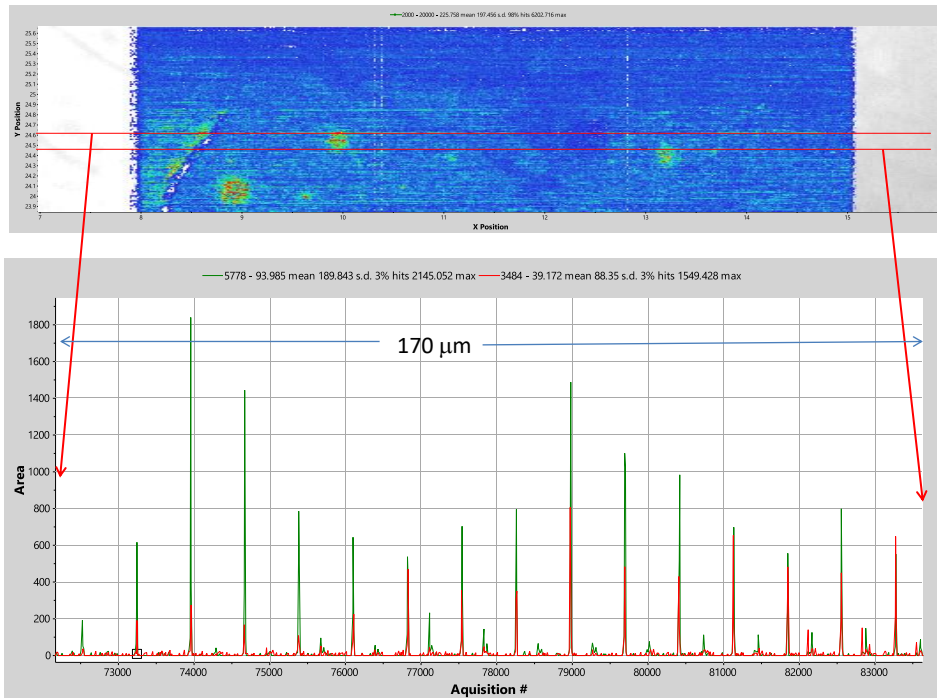


Figure 4. Upper panel is top portion of image in Figure 1A showing the vertical portion covering Islet 1 and picking up the top edge of Islet 2.

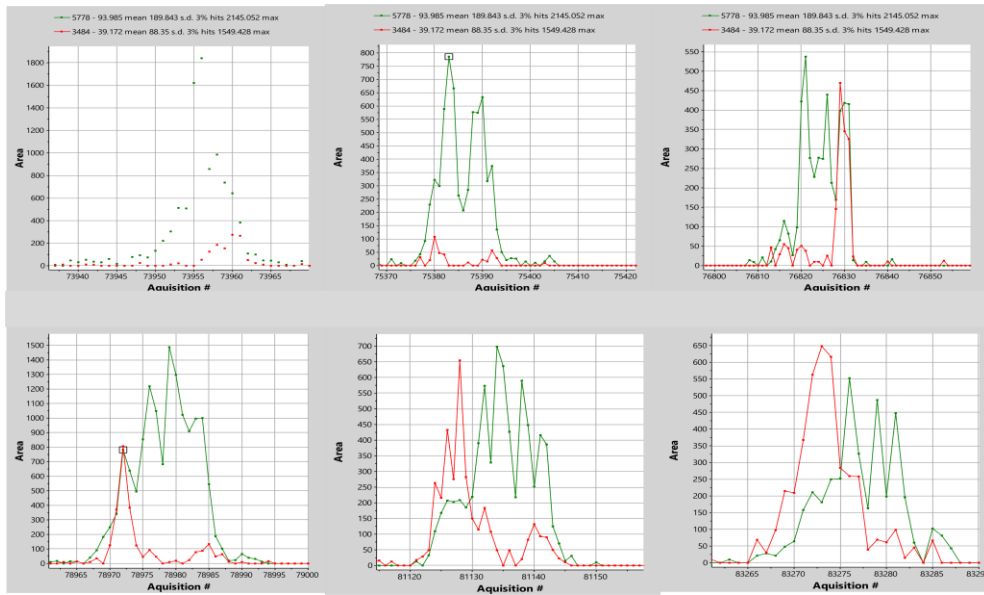


Figure 5. Expanded view of 6 passes across Islet 1 from near top (upper left) to near bottom (lower right)

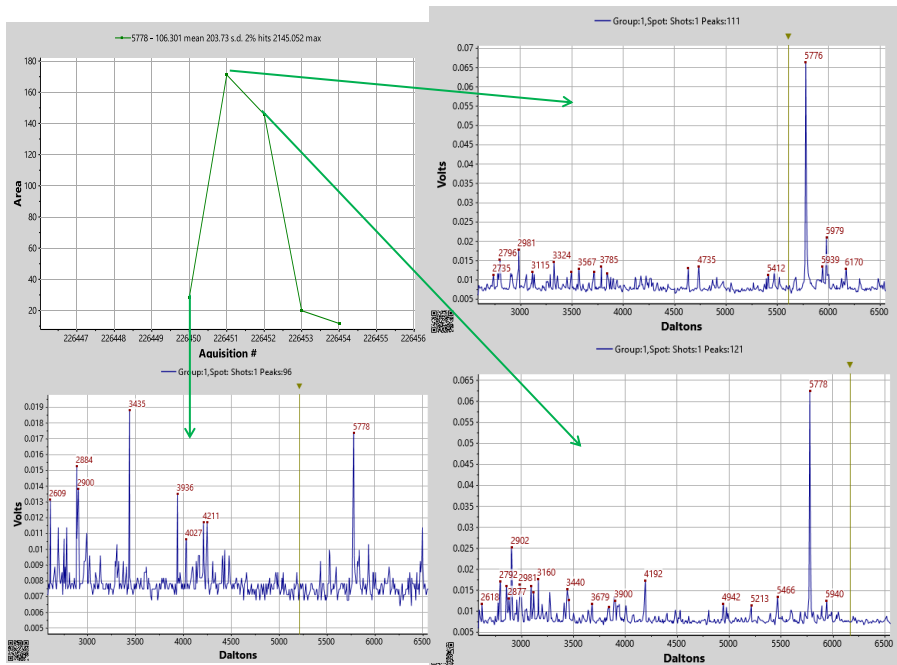


Figure 6. Image and spectra from what appears to be a single isolated beta cell. Location is indicated by arrow in Figure 2.

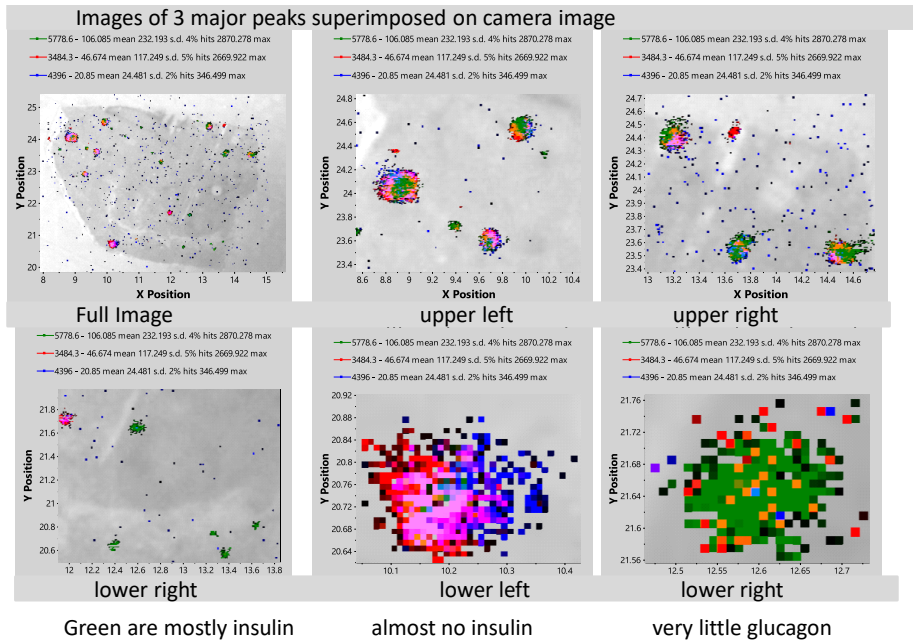
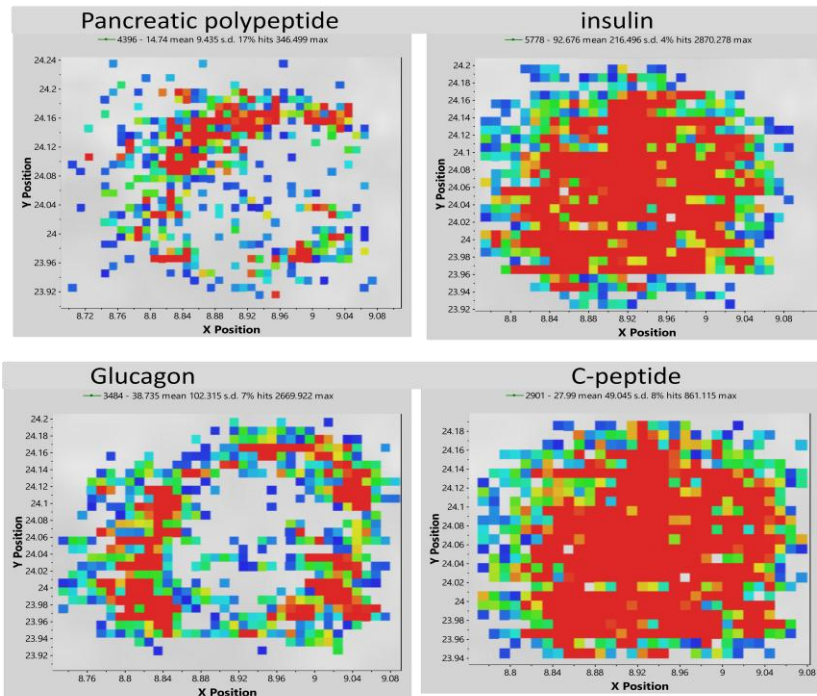
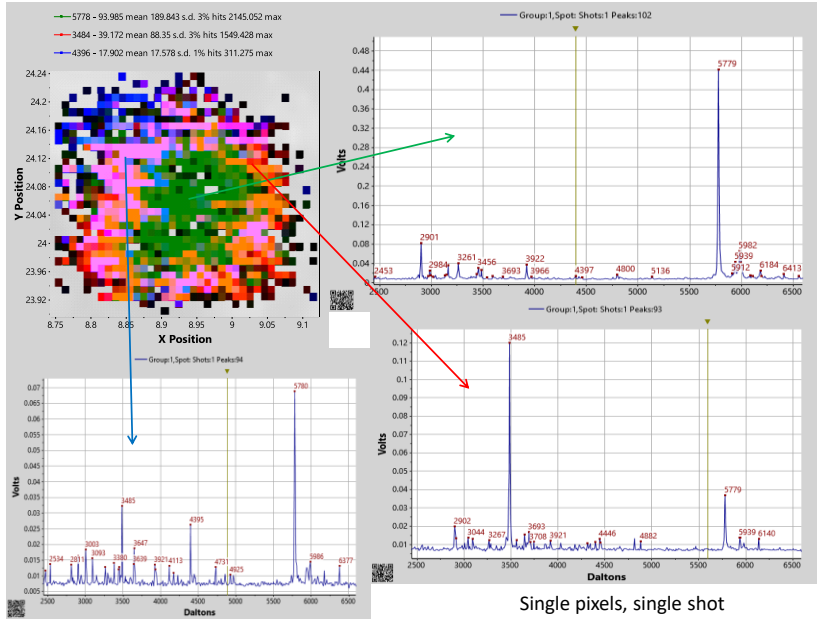


Figure 7. Expanded views showing more details of selected islets with insulin (green), glucagon (red), and pancreatic polypeptide (blue).



Heat maps of individual peptides – red high intensity, blue low

Figure 8. Individual images from Islet 3 for peptides that are found almost exclusively in the Islets



Single pixels, single shot

Figure 9. Spectra from selected single pixels, green (insulin), red (glucagon), blue (PPT). C-peptide at m/z 2901 is also detected in all of these.

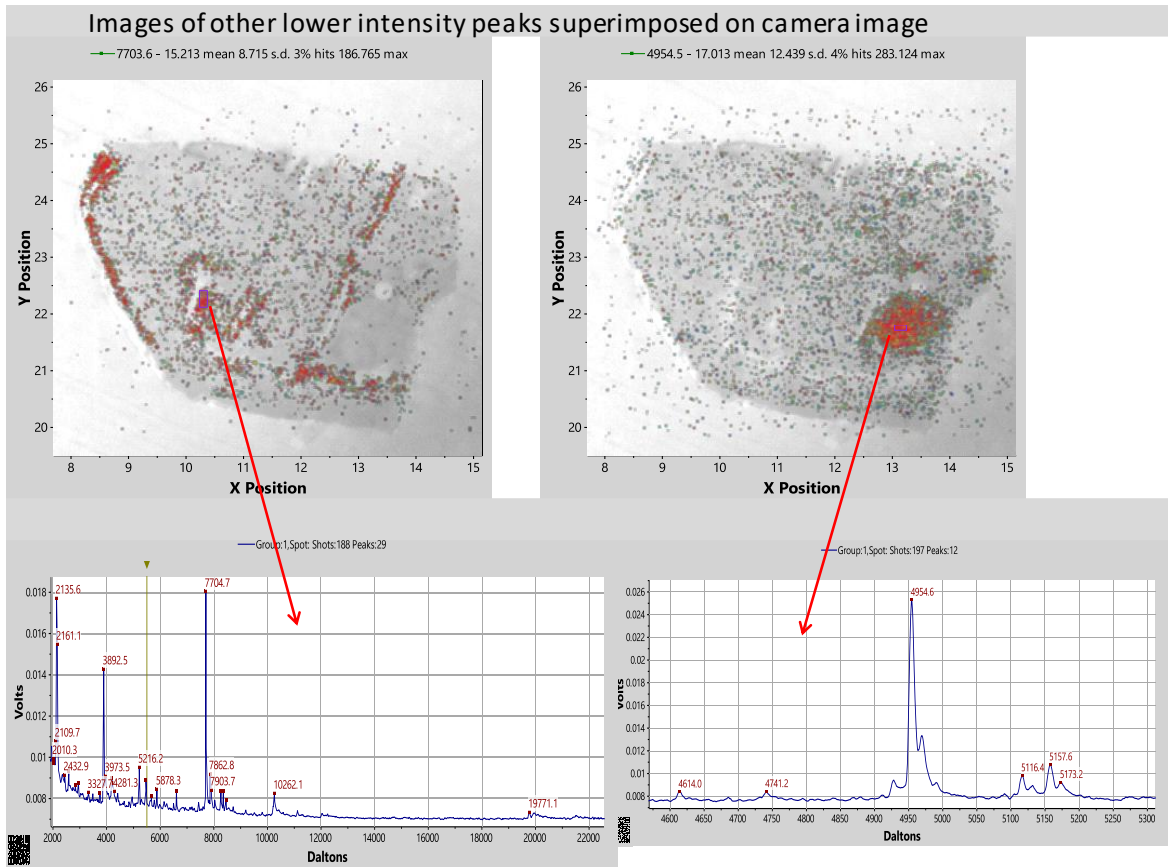


Figure 10. Example of spectra from other portions of the pancreas.

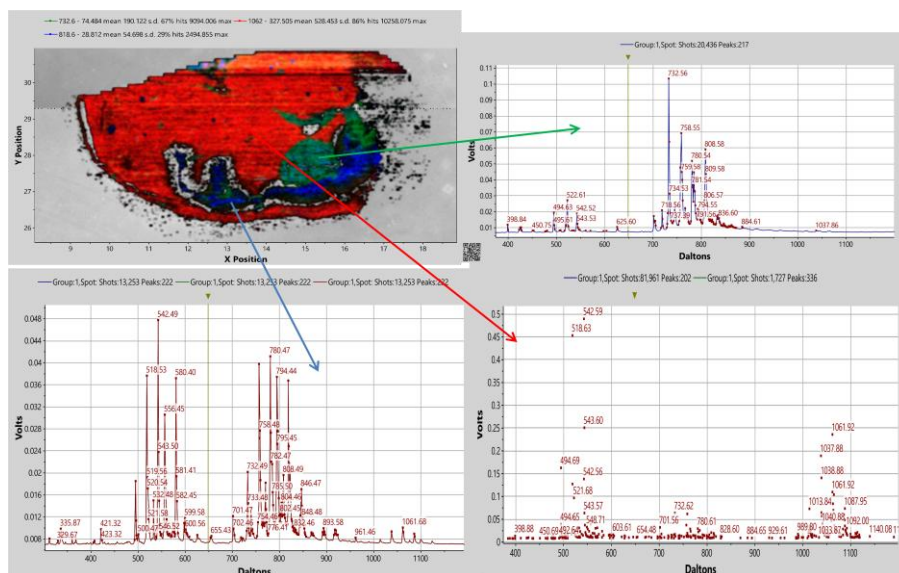


Figure 11. Lipid image from a different porcine pancreatic tissue section

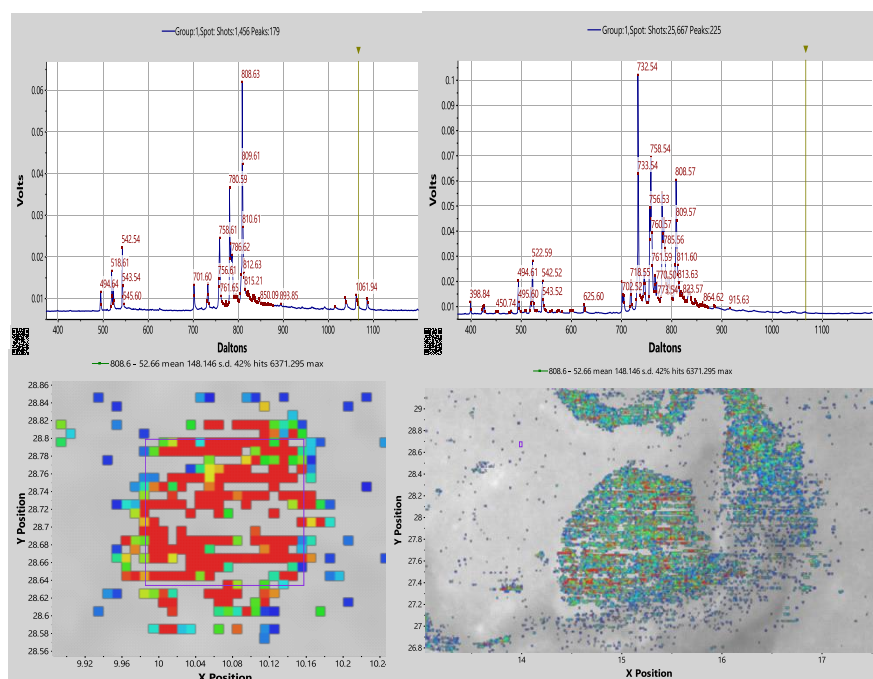


Figure 12. Lipid image and spectrum from an Islet of Langerhans (left) and another portion of the pancreas (right)

Acknowledgement: Porcine pancreas 12 um tissues sections were supplied pre- mounted onto ITO coated microscope slides by Prof Ron Heeren European institute for molecular imaging, (M4I) at Maastricht University Netherlands.